Improved functionality of hepatic spheroids cultured in acoustic levitation compared to existing 2D and 3D models

Lucile Rabiet, Nathan Jeger-Madiot, Duván Rojas García, Lucie Tosca, Gérard Tachdjian, Rémy Agniel, Jérôme Larghero, Jean-Luc Aider, Lousineh Arakelian, Sabrina Kellouche

Improved functionality of hepatic spheroids cultured in acoustic levitation compared to existing 2D and 3D models

Lucile Rabiet[1,2,*], Nathan Jeger-Madiot[1], Duván Rojas García[1], Lucie Tosca[3], Gérard Tachdjian[3], Sabrina Kellouche[4], Rémy Agniel[4], Jérôme Larghero[2], Jean-Luc Aider[1,*], and Lousineh Arakelian[2,*]

[1]Laboratoire Physique et Mécanique des Milieux Hétérogènes (PMMH), CNRS, ESPCI, 7 Quai Saint-Bernard, Paris, 75005, France
[2]Inserm U976, CIC-BT CBT501, AP-HP, Université Paris-Cité, Hôpital Saint-Louis, 1 avenue Claude Vellefaux, Paris, 75010, France
[3]Service Histologie Embryologie Cytogénomique, Hôpital Antoine Béclère, 157 Rue de la Porte de Trivaux, Clamart, 92140, France
[4]Laboratoire ERRMECe, Maison Internationale de la Recherche, CY Cergy Paris Université, 1 rue Descartes, Neuville-sur-Oise, 95000, France
[*]lucile.rabiet@gmail.com, jean-luc.aider@espci.psl.eu, lousineh.arakelian@aphp.fr

ABSTRACT

Hepatic spheroids are of high interest in basic research, drug discovery and cell therapy. Existing methods for spheroid culture present advantages and drawbacks. An alternative technology is explored: the hepatic spheroid formation and culture in an acoustofluidic chip, using HepaRG cell line. Spheroid formation and morphology, cell viability, genetic stability, and hepatic functions are analyzed after six days of culture in acoustic levitation. They are compared to 2D culture and non-levitated 3D cultures. Sizes of the 25 spheroids created in a single acoustofluidic microphysiological system are homogeneous. The acoustic parameters in our system do not induce cell mortality nor DNA damage. Spheroids are cohesive and dense. From a functional point of view, hepatic spheroids obtained by acoustic levitation exhibit polarity markers, secrete albumin and express hepatic genes at higher levels compared to 2D and low attachment 3D cultures. In conclusion, this microphysiological system proves not only to be suitable for long-term culture of hepatic spheroids, but also to favor differentiation and functionality within 6 days of culture.

Introduction

The liver is a vital organ with major properties, including protein synthesis and secretion, ion storage, and xenobiotics detoxification[1,2]. Despite its unique regenerative capacities in vivo,[3] isolated primary hepatocyctes are rapidy depolarized, lose their functionality and long term viability in vitro, in 2D culture[4].

Other hepatic cell models, including iPSC derived hepatoblasts and hepatic cell lines are also used for research purposes[5]. Among these cell lines, the bipotent HepaRG is of high interest[6]. In standard non-confluent 2D culture conditions, these cells proliferate and remain undifferentiated. At high confluence, cells differentiate along two sub-populations of hepatocyte-like and cholangiocyte-like cells. When further treated with dimethyl sulfoxide (DMSO), many genes including those of the detoxification enzymes are induced[7–9]. These properties have made HepaRG a useful tool for drug screening and basic research[10].

It has been shown that 3D culture models including spheroids and organoids improve hepatic cell functionality[11] and are promising tools for basic research, as well as drug screening. In vitro 3D cultures have been shown to be beneficial for both primary hepatocytes and hepatic cell lines[12,13].

Several techniques have been developed to create spheroids, such as suspension cultures, hanging drops, low attachment surfaces, scaffolds, microgravity, microphysiological systems or magnetic levitation[14,15]. Otherwise promising, all these methods still face some of the following hurdles: heterogeneity in size, labor-intensive procedure, low throughput, poorly defined matrices and hydrogels, low cellular functionality, or a lack of technological maturity[16–18]. These drawbacks have slowed down the use of spheroids in the interested fields, such as cell therapy[19–21] or drug development pipelines[22,23].

Acoustic levitation represents an innovative technique for spheroid formation. It implies the use of ultrasound waves that,

when reflected, create acoustic nodes that can trap small particles, as well as cells[24,25]. In our previous studies, we showed evidence that acoustic levitation allowed culturing different cell types, including HepaRG, up to 60 hours,[26,27] keeping them viable and allowing them to self-organize into spheroids. In the current study, HepaRG were cultivated in acoustic levitation for a longer period of time and cell viability, genetic stability and functionality were evaluated. Spheroids obtained in acoustic levitation were compared to 2D cultures and spheroids obtained in ultra-low attachment (ULA) plates.

Results

0.1 Comparative Morphological Analysis and Size Reproducibility Confirmation

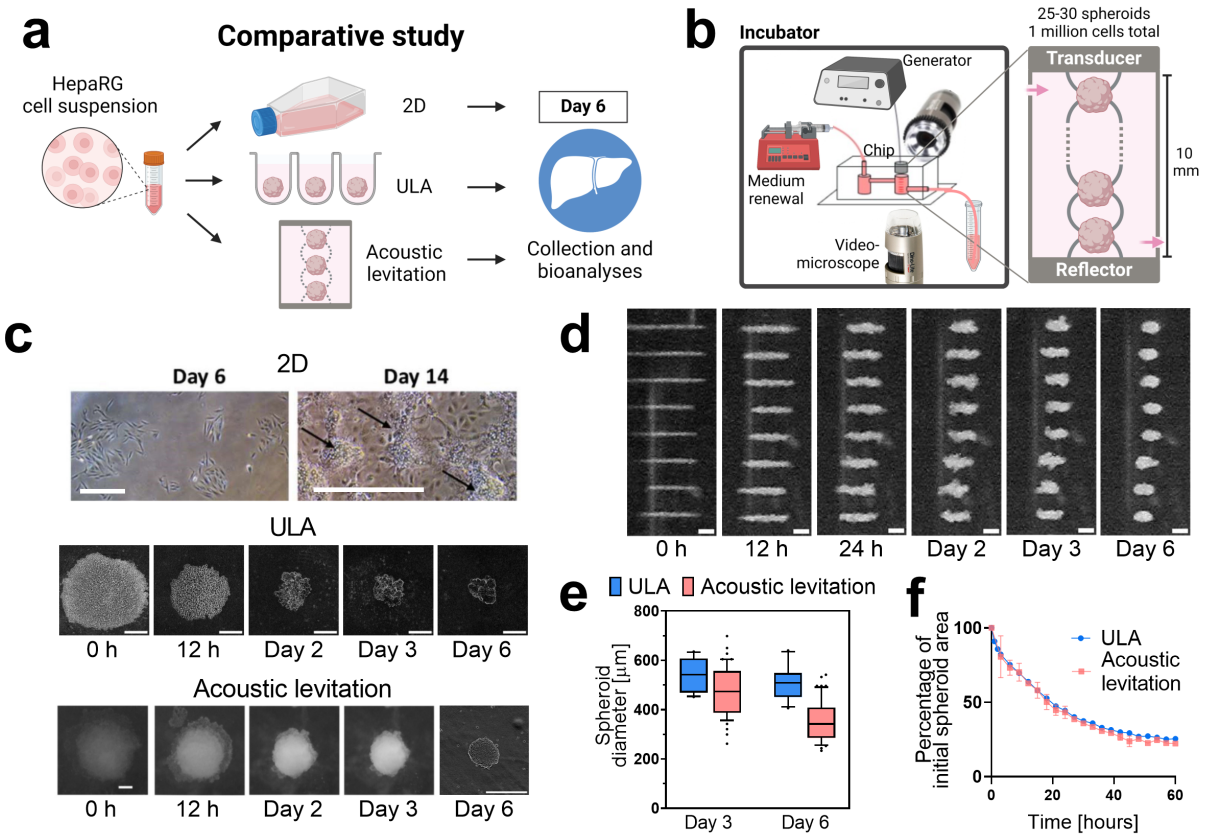

Figure 1. Comparative study during 6 days of cell culture. a) Schematic of workflow in 2D, ultra-low attachment and acoustic levitation. Created with BioRender.com. b) Schematic of the acoustofluidics setup for acoustic levitation. c) Morphology of HepaRG cultures, viewed from the top: in 2D at low confluence at day 6, and at high confluence at day 14 (arrows represent differentiated hepatocyte-like cells); in ULA dishes; and in acoustic levitation. Scale bars: 400 μm. d) Side-view of HepaRG spheroids in acoustic levitation. Scale bars: 200 μm. e) Distribution of diameters, showing size homogeneity of the spheroids. Middle line is plotted at the median, the box extends from the 25th to 75th percentiles and whiskers show 10-90 percentiles, n=12 for ULA and n=50 for acoustic levitation. f) Dynamics of spheroid formation in ultra-low attachment dishes and in acoustic levitation, calculated by percentage of initial spheroid area (from top-view). Error bars show mean $\pm$ SEM, n=12 for ULA and n=2 for acoustic levitation.

HepaRG cells were successfully cultured in 2D, in ULA and in acoustic levitation during 6 days (**Figure 1**a). Long-term culture in levitation was performed inside an incubator, with precise control of flow and of acoustic radiation force (ARF) and constant visual monitoring (Figure 1b). All cultures were imaged from the top (Figure 1c) and cultures in acoustic levitation were also imaged from the side (Figure 1d). As observed previously,[26,27] these cells organized themselves into spheroids in levitation. Spheroid formation was also obtained with HepaRG cells cultured in ultra-low attachment plates, whereas, in 2D cultures, cells grew in a monolayer as expected (Figure 1c). In 2D, non-confluent HepaRG cells had an elongated aspect, whereas, at high confluence, two subpopulations of hepatocyte-like and cholangiocyte-like cells could be observed (Figure

1c). Sizes and shapes of levitated spheroids were similar inside one acoustofluidic chip, and this homogeneity was observed throughout the self-organization (Figure 1d). Spheroids' diameters were homogeneous in levitation and comparable to ULA spheroids (Figure 1e). The dynamics of the self-organization into spheroids in acoustic levitation and ultra-low attachment plates were comparable, showing similar compaction rates (Figure 1f). Levitated spheroids remained cohesive after removal from the acoustofluidic chip, at day 6 (Figure 1c).

0.2 Levitated Spheroids Maintain a High Viability and Retain Their Bipotent Potential

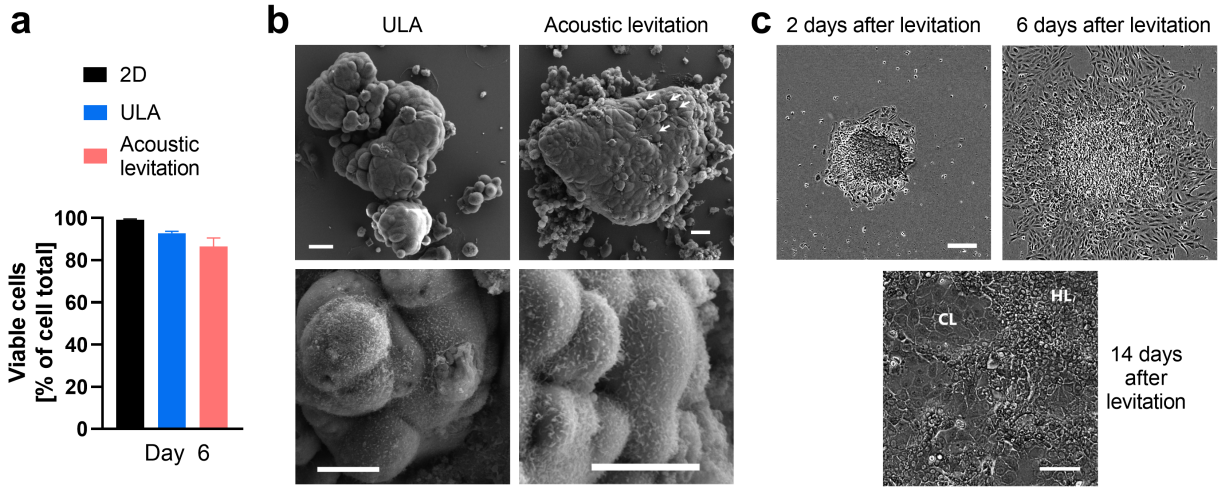

Figure 2. Validation of spheroid viability, adhesion and bipotent potential. a) Cell viability evaluated by flow cytometry after dissociation and Live/Dead staining. Error bars show mean ± s.d., n=3. b) Scanning electron microscopy (SEM) images of spheroids obtained in ultra-low attachment dishes or in acoustic levitation. Arrows indicate microchannels at the surface of the spheroids. Scale bars: 20 μm (upper row) and 2 μm (bottom row). c) Adhesion of HepaRG spheroids formed in acoustic levitation to a plastic culture flask. After initial proliferation, a bipotent phenotype (CL: cholangiocyte-like and HL: hepatocyte-like) is observed by optical microscopy, in a confluent cell monolayer, 14 days after the end of the levitation. Scale bars: 200 μm (upper row) and 50 μm (bottom row).

A direct viability assay performed on dissociated cells with the Live/Dead kit showed that adherent 2D cultures were almost 100% viable during the total period of 6 days of culture. The viability of cells in the spheroids formed in acoustic levitation and in ultra-low attachment plates were comparable (**Figure 2**a).

Scanning electron microscopy (SEM) was performed on spheroids that attached to coverslips after the initial 6 days of culture. Spheroids formed in ultra-low attachment 24-well plates were more heterogeneous in shape and size. Only the smaller non-levitated spheroids were able to adhere to the cover glasses whereas almost all levitated samples attached. The results revealed that levitated spheroids were more compact than ULA spheroids (Figure 2b). Tight interactions were observed between adjacent cells. Microchannels were spotted in between cells, at the surface of the levitated and non-levitated spheroids (Figure 2b, arrows, upper row). Such pores might suggest the presence of apical biliary canaliculi. Micro-villi structures typical of hepatic cells were observed in both levitated and non-levitated spheroids (Figure 2b, bottom row). Finally, when seeded on plastic, spheroids obtained by acoustic levitation and in ultra-low attachment plates were both able to adhere, spread and proliferate. Upon high confluence, after two weeks of culture, cells spread from spheroids differentiated into hepatocyte-like and cholangiocyte-like cells, indicating the preservation of their bipotency (Figure 2c).

0.3 Acoustic Levitation Does Not Disrupt the Genetic Stability of HepaRG Cells

0.3.1 The HepaRG Karyotype is Unaffected by 6 days of Acoustic Levitation

A preliminary karyotype analysis was performed on native HepaRG cells cultures in 2D, to study their basic characteristics. Analysis showed an abnormal karyotype with a supernumerary chromosome 7 of abnormal structure, and a derivative chromosome of a translocation between chromosome 12 and chromosome 22, resulting in the loss of chromosome 12 short arm (**Figure 3**a). These results are in accordance with the previous description of the cell line: 46,XX,+del(7)(q11;q21)inv(7)(q21q36),-der22t(12;22)(p11;q11)[6]. This sample served as control for the comparison of other culture conditions. HepaRG cells after 6 days of culture in 2D monolayers, in ultra-low attachment plates or in acoustic levitation, followed by 7 days of 2D amplification, showed similar results, without additional chromosomal alterations.

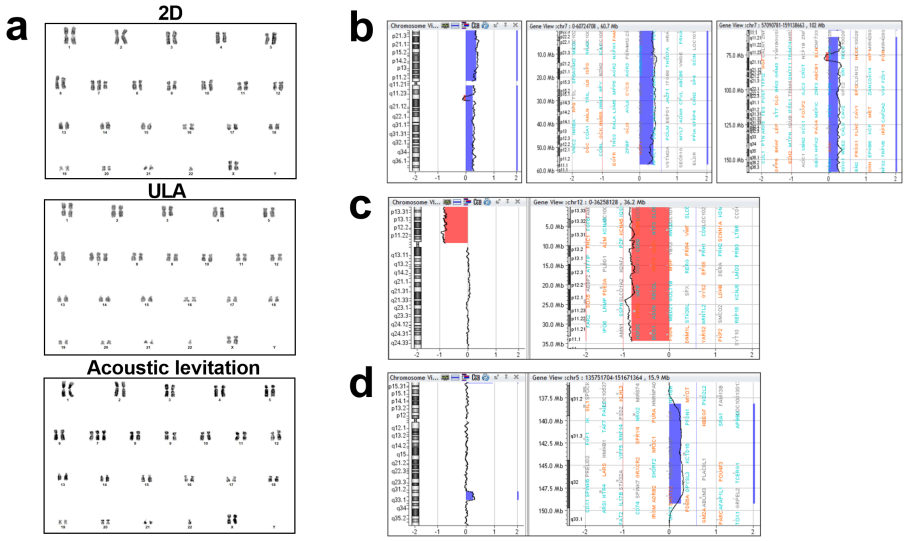

Figure 3. Genetic stability of the three culture systems. a) G-banded standard analysis of the HepaRG karyotype. The three culture models resulted in a female karyotype with an additional chromosome 7, a structural abnormality on one chromosome 12, and a missing chromosome 22 (arrows). b-d) Array CGH results on native HepaRG genomic DNA. b) Chromosome 7 profile with a complete trisomy and an interstitial deletion 7q11.23q21.11 of 6.45 Mb encompassing 49 RefSeq genes. View of whole chromosome 7 (left panel), short arm (middle panel), and long arm (right panel) ratio plots. c) Chromosome 12 profile with a monosomy 12p of 34.16 Mb encompassing 329 RefSeq genes. View of whole chromosome 12 (left panel) and short arm (right panel) ratio plots. d) Chromosome 5 profile with an interstitial duplication 5q31.2q32 of 11.14 Mb encompassing 148 RefSeq genes. View of whole chromosome 5 (left panel) and distal 5q region (right panel) ratio plots.

0.3.2 Array CGH

Array comparative genomic hybridization (CGH) on native HepaRG cells revealed a complete trisomy 7 (chr7:65,558-159,118,566, hg19) associated with an interstitial deletion 7q11.23q21.11 (chr7:73,265,298-79,725,034, hg19) of 6.45 Mb (Figure 3b), and a monosomy 12p13.33p11.1 (chr12:194,249-34,360,030, hg19) of 34.16 Mb (Figure 3c). An additional interstitial duplication 5q31.2q32 (chr5:138,139,653-149,283,415) of 11.14 Mb was observed (Figure 3d). These results were in agreement with the karyotype and previous description[6]. The analysis of HepaRG cells after 6 days of culture in 2D monolayers, in ultra-low attachment plates or in acoustic levitation, followed by 7 days of 2D amplification, showed no further relevant copy number variation (CNV).

Both karyotype and array CGH analysis confirmed that ultrasounds used for acoustic levitation did not induce DNA damage or alteration.

0.4 Levitated Spheroids are Polarized and Functional

Albumin (ALB) secretion is a hallmark of liver functionality. Therefore, ALB gene expression and protein secretion were quantified by RT-qPCR and by ELISA, respectively (**Figure 4**a). ALB was not expressed in 2D non-confluent cultures whereas it was significantly overexpressed in spheroids formed in ultra-low attachment plates (mean RQ 6.2). This expression was even stronger in levitated spheroids (mean RQ 15.8). Albumin quantification by ELISA confirmed these results at protein secretion level. No albumin was detected in 2D non-confluent cultures' supernatant whereas the total quantity detected in ULA spheroids culture medium was 2.7 μg and for levitated spheroids 10.53 μg.

The same overexpression tendency of polarization markers including MRP2, MRP3 and BSEP was observed in spheroids compared to non-confluent 2D HepaRG cells (Figure 4b).

As for the expression of nuclear receptors, no difference was detected for AhR between the three models, whereas PXR and CAR were strongly overexpressed in the spheroids. CAR was overexpressed 45.5 folds in ULA spheroids and 72.4 folds in levitated ones (Figure 4c).

Drug-metabolizing and urea cycle enzymes, including Cyp1A1, Cyp1A2, CYP2C9, Cyp2E1, Cyp3A4 and ARG1 were strongly overexpressed in spheroids compared to non-confluent 2D cultures. These gene expressions were much stronger in levitated spheroids than ULA ones (Figure 4c).

These results indicate a more mature and functional profile of spheroids compared to 2D samples.

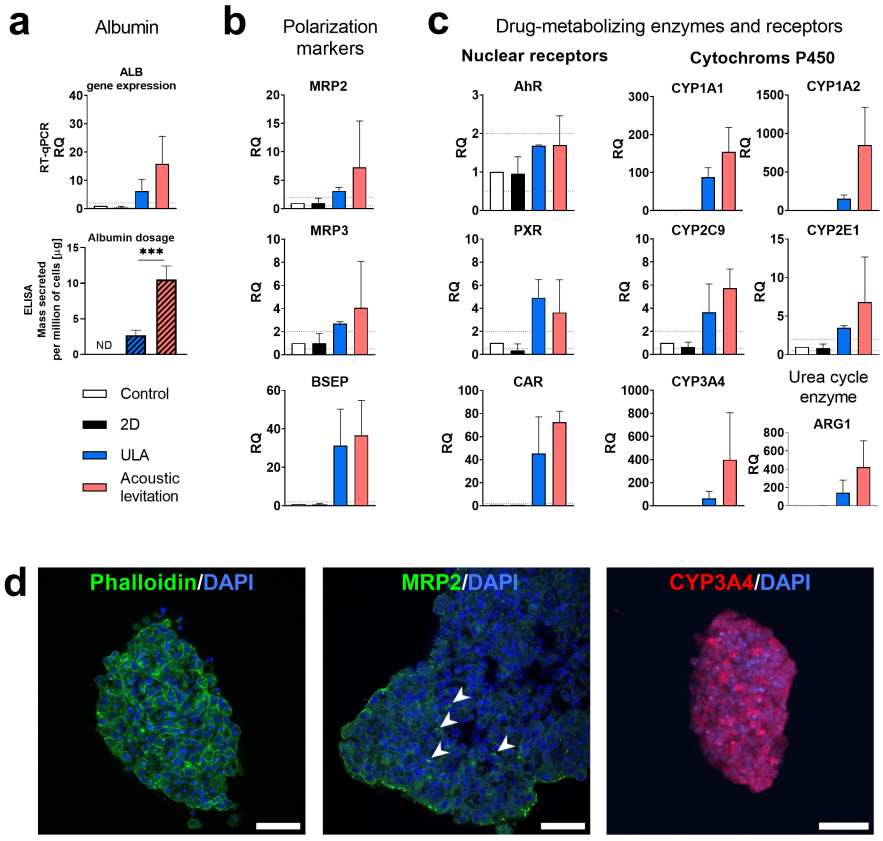

Figure 4. Hepatic cell functionality after 6 days in one of the three culture models. a) Albumin gene expression and protein secretion evaluated by RT-qPCR and ELISA respectively. b-c) Gene expression (RT-qPCR) of polarization markers, nuclear receptors, CYP450 drug-metabolizing and urea cycle enzymes. Error bars show mean ± s.d., n=3. d) Immunofluorescence of cryosectioned spheroids, after 6 days of acoustic levitation. Spheroids were stained for the F-actin label phalloidin (green, left), the polarization marker MRP2 (green, middle) or the drug-metabolizing enzyme CYP3A4 (red, right). All cryosections were stained with DAPI (blue). Arrows indicate intraspheroidal MRP2 clusters. Scale bars: 25 μm (middle), 50 μm (left and right).

Immunostaining was also performed on levitated spheroids. Phalloidin staining showed a cohesive spheroid, with the actin cytoskeleton mainly concentrated at cell cortex. Moreover, we showed that spheroids expressed Cyp3A4, and that MRP2 was found at the surface of the spheroid, as well as more scarcely inside, demonstrating a stronger polarization at the surface compared to the core of the spheroids (Figure 4d).

Discussion

Our acoustofluidic device was first used as a tool to form rapidly cohesive spheroids, from an initial cell suspension. The formation of spheroids in acoustic levitation was comparable to the formation of spheroids in standard low attachment plates. As previously reported, in acoustic levitation, self-organization relied strongly on the cell type characteristics[27]. Therefore, it is expected that levitated and non-levitated spheroids displayed similar dynamics of formation. Nevertheless, a higher circularity was obtained in acoustic levitation, which might be explained by the influence of the transverse component of the ARF. The impact of this force has been reported in previous works[28,29]. This could also be observed by SEM, which showed that levitated spheroids were more compact than ULA ones. Our study highlighted a satisfactory homogeneity in shape and size of levitated spheroids. It is comparable to the reproducibility of spheroids formed in low attachment 96-well plates, a technique that is well-known for its reproducibility[30]. Spheroids obtained in acoustic levitation were rapidly cohesive, and remained this way even after interruption of the ultrasonic trapping. Long-term culture in acoustic levitation, up to 6 days, did not affect the cohesiveness of the spheroids, thus assuring biomimetic cell-cell interactions.

We previously reported the proof of concept of cell culture in acoustic levitation for 24 hours[26]. Nevertheless, prolonged exposition to ultrasounds during 6 days brought specific concerns such as increase in temperature, creation of pores in the

plasma membrane, shear stress, cell lysis or DNA damage[31,32].

These effects are generally witnessed with high intensity ultrasounds, which is clearly not the case for our system, where low intensity ultrasounds were used (voltage < 5 V_{pp} and power < 0.1 W) allowing a very gentle manipulation of cells. Viability of the levitated spheroids was excellent and comparable with 2D and ULA controls. Genetic stability was maintained, confirming that acoustic levitation did not induce further chromosomal damage or genetic alterations. This genetic stability is an important point, especially if this culture system is further developed for being used for therapeutic purposes[33,34].

HepaRG cells are an excellent tool for drug testing. However, in order to differentiate in 2D culture, they have to attain a very high confluence, for at least 14 days[35]. Furthermore, culture in the presence of DMSO is required to induce detoxification enzymes, but this stimulation is not stable overtime and enzyme expression levels drop upon removal of DMSO. Therefore, the development of technologies allowing a DMSO-free and stable cell differentiation could be beneficial for drug screening purposes. Our results showed that 3D culture of HepaRG as spheroids induced a strong overexpression of detoxification enzymes as well as polarization markers, compared to nonconfluent 2D cultures. This effect was much emphasized in levitated spheroids. This could be partly due to a rapid cell aggregation in acoustic levitation, mimicking a high confluence. It has thus been reported that a stable overexpression of CAR receptor reduces the requirement for DMSO treatment of HepaRG, for induced drug metabolism[36]. These results indicate that there may be a chain of gene expression control between CAR and metabolic enzymes, which is stable overtime in 3D HepaRG cultures.

In conclusion, we show that acoustic levitation is an innovative tool well adapted to HepaRG long-term and gentle cell culture. It allows a rapid aggregation of cells, leading to their fast and increased maturation, without inducing any genetic damage. When compared to classic ULA spheroids, these levitated spheroids had globally a much higher expression of liver specific genes. In the future, it would be interesting to culture other hepatic models such as primary hepatocytes or iPSC-derived hepatoblasts, in order to study the effects of acoustic levitation on cell proliferation and functionality. This innovative cell culture tool could be up-scaled for the development of reproducible hepatic spheroids that could be used for drug screening, disease modeling or cell therapy.

Methods

HepaRG Culture and Amplification

Cells and spheroids were cultivated in incubators at 37°C and 5% CO_2. For amplification, HepaRG cells (Biopredic, St. Grégoire, France) were cultivated in basal hepatic cell medium (Biopredic) with 10% of HepaRG growth medium supplemented with antibiotics. The initial cell density was $2.8{\times}10^4$ cells cm^{-2}. Culture medium was renewed every 3 days. Every 14 days, cells were detached and passaged using 0.25% trypsin + EDTA (Gibco, UK).

Acoustic levitation

To create an acoustic force field inside a cavity, one has to create an acoustic standing wave by placing a reflector facing the transducer at a distance h matching the resonance condition ($h = n\lambda_{ac}/2$, with λ_{ac} the acoustic wavelength). The particles or cells inside the cavity are then submitted to the acoustic radiation force (ARF). The axial component of the ARF (F_{ac}) forces them to move toward the acoustic pressure nodes (levitation planes).

The ARF can be written as[37]:

$$F_{ac} = \frac{\pi}{4} E_0 \, k \, d_p^3 \, F_Y \, \sin(2kz) \, e_z \tag{1}$$

where E_0 is the mean acoustic energy density, d_p the diameter of the object, F_Y the acoustic contrast factor and k the acoustic wave number[38]. This expression is valid for spherical particles much smaller than the acoustic wavelength (Rayleigh approximation). Usually, one can consider that the acoustic levitation plane is located at the acoustic pressure node, but for dense and / or large objects, this condition is not necessarily verified and the axial position of the levitation planes may be lower than the acoustic pressure node. These non-standard conditions can lead to the triggering of self-acoustophoresis of metallic nanorods[39] or displacement of large levitated objects[40]. In our case, once the spheroids have been formed in levitation, they remain at a stable equilibrium position.

Acoustofluidic Chips

The acoustofluidic chips were fabricated in polydimethylsiloxane (PDMS, 1:10 curing agent:base ratio, RTV 615, Neyco, Vanves), a transparent, gas permeable and biocompatible material that does not strongly reflect acoustic waves. PDMS was poured in a plexiglass mold, heated at 70°C for 24h, then bonded with a plasma cleaner on a microscope glass slide (acoustic reflector). Each acoustofluidic chip is comprised of two chambers: an acoustofluidic well and its preceding passive bubble trap. There are connected by PDMS channels. The formation of bubble is non existent inside the well. However, due to the

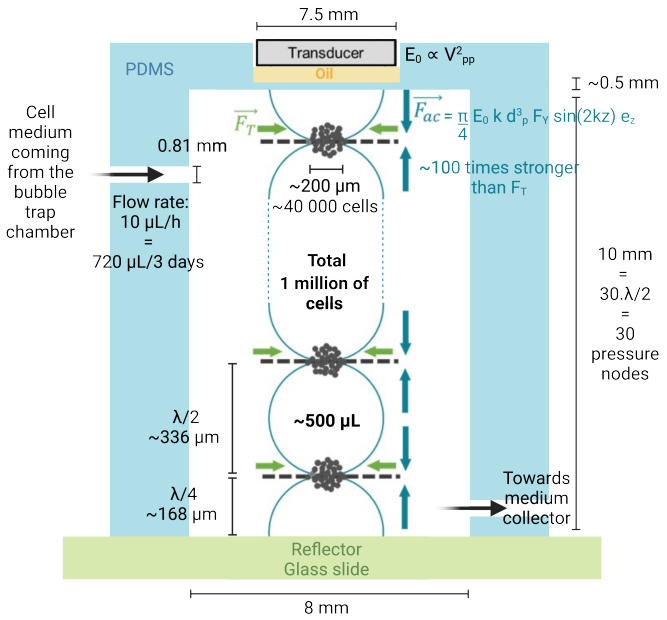

Figure 5. Schematic of the acoustofluidic well used in the present study to form and culture HepaRG spheroids over 6 days. The walls of the well are made of PDMS. An oil layer is used as a matching layer between the upper wall of the well and the transducer. The reflector facing the transducer is a glass slide. A constant flow rate is applied, allowing a total renewal of the medium after 3 days. The typical sizes of spheroids, as well as the internode distance obtained with a 2.2 MHz acoustic wave, are also displayed on the schematic.

continuous medium renewal, bubbles frequently arrive with the flow and are stopped inside the passive bubble trap chamber (Figure 1b) before arriving in contact with the cells or the acoustic field. The bubble trap is a cylindrical well (height $h = 12$ mm and diameter $d = 5$ mm), where gaz bubble are trapped at the top, while liquid medium exits at the bottom.

Formation and Culture of Spheroids in Acoustic Levitation

In our acoustofluidic chip (**Figure 5**), a 2 MHz ultrasound broadband transducer was used to create a multi-modes acoustic standing wave in a $h = 10$ mm high well. Ultrasonic standing waves of a few megahertz can produce an Acoustic Radiation Force (ARF) that can be used to manipulate small particles as well as mammalian cells. The acoustic frequency F_{ac} (and corresponding acoustic wavelength λ_{ac}) was tuned to match the resonance condition ($h = n\lambda_{ac}/2$). One million cells were injected in each chip. Ultrasonic transducers (SignalProcessing ™) were powered by a waveform generator (Handyscope HS5, TiePie Engineering™) with a sinusoidal waveform of constant amplitude of $A = 3.5$ V_{pp}, which is the smallest possible amplitude to maintain the spheroids in levitation.

The acoustic frequency used was $F_{ac} = 2.2$ MHz for these resonant cavities, a value contained in the levitation range of 1.5 to 2.5 MHz, as shown in previous studies[41,42]. After emission by the transducer, the acoustic wave travels through oil (acoustic matching layer), a PDMS membrane and the bulk of the well filled with cell medium, before reaching a glass slide, which plays the role of the reflector on the other side of the well (Figure 5). The height of the cavities ($h = 10$ mm) lead to the formation of 30 levitation planes, i.e. 25 to 30 spheroids per chip (Supplementary Figure 1). Levitated spheroids were formed and cultured in eight chips in parallel.

A syringe pump perfused the chip with a constant flow rate of 10 μL h^{-1} (Pump 11 Elite, Harvard Apparatus™) in order to renew the medium every three days. Timelapses showing the evolution of the spheroids inside the chip were obtained using Dino-Lite Pro 630-1165 USB Microscopes (Dinolite™). Snapshots were taken every 10 minutes during the duration of the culture. After 6 days, the ultrasound were turned off and the spheroids were collected from the chip by aspiration. They were immediately transferred into a 96-well plate and were placed in an Incucyte S3 imaging system (Sartorius™) for immediate imaging of the top view of the spheroids.

Geometrical Analysis

In order to quantify the dynamics of formation of the spheroids as well as the possible evolution of their size and shape over the time of the culture, diameter of the spheroids were computed from the snapshots using the ImageJ software. To characterize the time evolution of the shape of the spheroids during the first three days, we computed the area from ImageJ analysis of the top views of the spheroids.

Cell Viability

Levitated spheroids were aspirated from the culture devices and were placed in a 15ml centrifugation tube (Falcon). ULA spheroids were also collected in 15 mL centrifugation tubes. Spheroids were centrifuged at 284 g for 5 minutes at 20°C and the supernatant was eliminated. Monolayers and spheroids were then dissociated into single cells with 0.25% trypsin during 15 minutes. After suspension in PBS (Eurobio, Courtaboeuf, France), all conditions were stained for 5 minutes with calcein and ethidium bromide (LIVE/DEAD mammalian viability kit, Montlucon, France). Viability of individual cells was evaluated by flow cytometry (Attune® NxT Acoustic Focusing Cytometer).

Scanning Electron Microscopy

After 6 days of culture, ULA spheroids or levitated spheroids were collected and placed on round cover glasses (12 mm diameter) inside a 24-well plates (Corning, Falcon, NY, USA) for 24 hours. Adherent spheroids were fixed with glutaraldehyde 2.5% and PFA 2%, diluted in cacodylate 0.1 M buffer. After dehydration in several ethanol baths of increasing concentration, supercritical drying with carbon dioxide was performed. Spheroids were coated with platinum 4 nm. The sample preparation preserved the 3D structure of the spheroids. Scanning electron microscopy was conducted using a field emission gun scanning electron microscope (GeminiSEM300, Carl Zeiss) with an acceleration voltage of 2 keV under high vacuum. Secondary electrons were collected. Scan speed and line averaging were adjusted during observation.

Spheroids Readhesion and Spreading on Plastic

After 6 days in levitation, spheroids were transferred in 96-well plates (Corning, Falcon, NY, USA) with fresh medium, and placed in an Incucyte S3 imaging system (Sartorius) at 37°C. Images were taken every 10 minutes during 14 days to assess the adhesive potential of levitated spheroids.

Genetic Stability

Genetic stability was evaluated by karyotype and array comparative genomic hybridization (CGH). Cells originating from the same culture batch were cultivated in acoustic levitation, in 24-well ultra-low attachment plates or in 25 mm^2 flasks during 6 days (three replicates for each), then cultivated in adhesive 6-well plates (Corning, Falcon, NY, USA) for amplification during 7 days.

Karyotype

While plates were still not confluent, 20 μL of colchicin (20 mg L^{-1} ; EUROBIO) were added in each 6-well plate well, followed by an incubation of 2 h at 37°C. Cells were detached with 0.25% trypsin during 5 minutes (37°C), transferred into a 15 mL tube and centrifuged at 284 *g* for 5 minutes at 20°C. Supernatant was replaced by 8 mL of preheated KCL 0.075 M and incubated during 20 min at 37°C. 2 mL of 4°C Carnoy (3:1 methanol:acetic acid) were added for prefixation of the samples. After centrifugation, the supernatant was eliminated and samples were fixed in 8 mL of Carnoy. Samples were kept at 4°C before analysis. Karyotype was studied using standard procedures (G-banding by using trypsin and Giemsa staining (GTG).

Array Comparative Genomic Hybridization (CGH)

Cells were dissociated with 0.25% trypsin during 5 minutes (37°C). DNA was extracted from the samples using Mini-Kit PureLink® Genomic DNA Kits K1820-02, according to the manufacturer's instructions, and eluted in 50 μL of PureLink Genomic Elution Buffer. DNA quantity and purity were evaluated using NanoDropLite (Thermo scientific™).

DNA integrity was assessed on a 1% agarose gel. Genomic imbalances were analyzed by array CGH using 180K oligonucleotide arrays (Agilent Technologies, Massy, France). Genomic DNAs from 2D cultures and spheroids were compared with native HepaRG genomic DNA. Hybridization was performed according to the manufacturer's protocol. Images were processed with Feature Extraction software (10.7.3.1), and data analysis was performed with Genomic Workbench V5.0.14 (Agilent Technologies). The genomic positions were determined using version 19, Build37 of the human Genome Browser (University of California, Santa Cruz, CA; http://genome.ucsc.edu/). The Aberration Detection Method 2 algorithm was used for statistical analysis. Copy number alterations were considered important if they were defined by four or more oligonucleotides and spanned at least 39 kb and were not identified in the Database of Genomic Variants (http://projects.tcag.ca/cgi-bin/variation/gbrowse/hg19).

Secreted Albumin Quantification

Supernatants of levitated samples (1 million of cells) were collected at the outlet of the chip during the 6 days of medium renewal. Supernatants of non-levitated samples (2D culture and ULA spheroids ; 1 million of cells) were collected during medium renewal at day 3 and day 6, and pooled. Albumin quantification in the supernatants was performed with Human Serum Albumin DuoSet ELISA (RnD Systems™), according to the manufacturer's instructions. The optical density at 450 nm was detected using a microplate reader (Varioskan™ LUX multimode, Thermo Scientific™, Waltham, MA USA). Supplemented HepaRG cell culture medium served as negative control. The concentration (μg mL^{-1}) was multiplied by the total volume of the supernatant in order to calculate the total albumin secreted by the cells (μg).

RNA Extraction

RNA extraction was performed based on a trizol/chloroform method. RNA quantity and purity were evaluated using NanoDropLite (Thermo scientific™). Gene expression was then evaluated by reverse transcription-quantitative polymerase chain reaction (RT-qPCR).

Reverse Transcription (RT)

RT was performed with 500 ng of RNA and high capacity cDNA reverse transcription kit (Thermofisher™) in 0.5 mL tubes (Easy strip Snap Tubes, Thermofisher™) in a SimpliAmp Thermal Cycler (Applied Biosystems), using the following program: 10 mins at 25°C, 120 mins at 37°C, 5 mins at 85°C, followed by a cooling step at 4°C.

Quantitative Polymerase Chain Reaction (qPCR)

The cDNAs were diluted to 1/50 in nuclease free water and were used for qPCR (5 ng of cDNA per well) with RNEasy Plus Mini Kit (Quiagen). TaqMan™ probes were used for the amplification. The reactions were performed in 384 reaction plates (Applied Biosystem™) in a final volume of 20 μL per well. The reagents were dispatched in the wells using an Epmotion 5073 robot (Eppendorf).The expression of genes related to polarity (apical cell membrane transporters), detoxification (nuclear receptors and cytochromes), albumin and the urea cycle were analyzed. RPLP0 was used as housekeeping gene. The list of the TaqMan™ probes used for these experiments are found in Table 1.

Table 1. TaqMan™ probes used for the qPCR analysis.

Gene symbol	Protein full name	Reference
RPLP0	Ribosomal protein lateral stalk subunit P0	Hs99999902
MRP2 / ABCC2	Multi-drug resistance protein 2	Hs00166123
MRP3 / ABCC3	Multi-drug resistance protein 3	Hs00978452
BSEP / ABCB11	Albumin	Hs00609411
AhR	Aryl Hydrocarbon Receptor	Hs00169233
PXR / NR1I2	Pregnane X receptor	Hs01114267
CAR / NR1I3	Constitutive androstane receptor	Hs00901571
CYP1A1	Cytochrome P450 family 1 subfamily A member 1	Hs01054796
CYP1A2	Cytochrome P450 family 1 subfamily A member 2	Hs00167927
CYP2C9	Cytochrome P450 family 2 subfamily C member 9	Hs02383631
CYP2E1	Cytochrome P450 family 2 subfamily E member 1	Hs00559367
CYP3A4	Cytochrome P450 family 3 subfamily A member 4	Hs00604506
ALB	Bile salt export pump	Hs00994811
ARG1	Arginase 1	Hs00163660

All results were expressed as relative quantification (RQ) compared to one of the control samples which consists of HepaRG cells cultivated during 6 days in 2D (initial seeding density of 28 000 cells cm^{-}2). Statistical test: t-test (n=3). An RQ difference of factor 2 was considered as significant.

Cryosection

Levitated spheroids at day 6 were fixed in PFA 4% during 30 min, then stored at 4°C in PBS. The supernatant was replaced by a 15 % sucrose (Sigma-Aldrich) solution in PBS for 1 h, then by a 30 % sucrose solution for 48 h. Spheroids were withdrawn from the sucrose solution, and deposited inside a silicon mold filled with $\approx$ 1 mL of optimal cutting temperature (OCT) cryofix gel (Biognost) cryo-embedding matrix. The samples were immediately placed on dry ice and frozen. Samples were removed from the mold, placed in cold 2 mL tubes and stored at -80°C. Spheroids were cut (25 μm sections) with a cryostat (Leica CM 1950) and deposited on polylysin-coated glass slides. Sections were stored at -80°C until staining.

Immunofluorescence

Samples were saturated and permeabilized for 15 min in PBS containing 3% bovine serum albumin (BSA) and 0.05% Triton, followed by a 30 min incubation in O.3M glycin. They were then incubated for 1 h with the primary antibodies (dilution 1:200, 200 μL per slide). After three washes in PBS-BSA and 0.1 % Tween-20, samples were incubated during 30 min with

phalloidin-FITC (1:500) or secondary antibodies (1:500). Cell nuclei were stained with DAPI (1:2000). After three washes, cover slides were mounted with ProLong^{TM} Gold antifade reagent (Life Technologies). The primary and secondary antibodies are listed in Table 2. Images were acquired using a confocal microscope LSM 780 system.

Table 2. Primary and secondary antibodies used for immunofluorescence.

Antibody	Supplier	Reference
Rabbit anti-CYP3A4	Invitrogen	PA1-343
Goat anti-rabbit IgG-Alexa Fluo™ 555	Invitrogen	A21428
Mouse anti-MRP2	Santa Cruz	SC-59609
Goat anti-mouse IgG1- Alexa Fluor™ 488	Invitrogen	A21121

References

1. Ehrlich, A., Duche, D., Ouedraogo, G. & Nahmias, Y. Challenges and Opportunities in the Design of Liver-on-Chip Microdevices. *Annu. Rev. Biomed. Eng.* **21**, 219–239, DOI: 10.1146/annurev-bioeng-060418-052305 (2019).
2. Liu, M. *et al.* State-of-the-art advancements in Liver-on-a-chip (LOC): Integrated biosensors for LOC. *Biosens. Bioelectron.* **218**, 114758, DOI: 10.1016/j.bios.2022.114758 (2022).
3. Michalopoulos, G. K. & Bhushan, B. Liver regeneration: Biological and pathological mechanisms and implications. *Nat. Rev. Gastroenterol. & Hepatol.* **18**, 40–55, DOI: 10.1038/s41575-020-0342-4 (2021).
4. Elaut, G. *et al.* Molecular mechanisms underlying the dedifferentiation process of isolated hepatocytes and their cultures. *Curr. Drug Metab.* **7**, 629–660, DOI: 10.2174/138920006778017759 (2006).
5. Zeilinger, K., Freyer, N., Damm, G., Seehofer, D. & Knöspel, F. Cell sources for in vitro human liver cell culture models. *Exp. Biol. Medicine (Maywood, N.J.)* **241**, 1684–1698, DOI: 10.1177/1535370216657448 (2016).
6. Gripon, P. *et al.* Infection of a human hepatoma cell line by hepatitis B virus. *Proc. Natl. Acad. Sci.* **99**, 15655–15660, DOI: 10.1073/pnas.232137699 (2002).
7. Le Vee, M. *et al.* Functional expression of sinusoidal and canalicular hepatic drug transporters in the differentiated human hepatoma HepaRG cell line. *Eur. J. Pharm. Sci. Off. J. Eur. Fed. for Pharm. Sci.* **28**, 109–117, DOI: 10.1016/j.ejps.2006.01.004 (2006).
8. Kanebratt, K. P. & Andersson, T. B. HepaRG cells as an in vitro model for evaluation of cytochrome P450 induction in humans. *Drug Metab. Dispos. The Biol. Fate Chem.* **36**, 137–145, DOI: 10.1124/dmd.107.017418 (2008).
9. Mayati, A. *et al.* Functional polarization of human hepatoma HepaRG cells in response to forskolin. *Sci. Reports* **8**, 16115, DOI: 10.1038/s41598-018-34421-8 (2018).
10. Kamalian, L. *et al.* The utility of HepaRG cells for bioenergetic investigation and detection of drug-induced mitochondrial toxicity. *Toxicol. vitro: an international journal published association with BIBRA* **53**, 136–147, DOI: 10.1016/j.tiv.2018.08.001 (2018).
11. Lauschke, V. M., Shafagh, R. Z., Hendriks, D. F. G. & Ingelman-Sundberg, M. 3D Primary Hepatocyte Culture Systems for Analyses of Liver Diseases, Drug Metabolism, and Toxicity: Emerging Culture Paradigms and Applications. *Biotechnol. J.* **14**, 1800347, DOI: 10.1002/biot.201800347 (2019).
12. Takahashi, Y. *et al.* 3D spheroid cultures improve the metabolic gene expression profiles of HepaRG cells. *Biosci. Reports* **35**, e00208, DOI: 10.1042/BSR20150034 (2015).
13. Vorrink, S. U. *et al.* Endogenous and xenobiotic metabolic stability of primary human hepatocytes in long-term 3D spheroid cultures revealed by a combination of targeted and untargeted metabolomics. *FASEB journal: official publication Fed. Am. Soc. for Exp. Biol.* **31**, 2696–2708, DOI: 10.1096/fj.201601375R (2017).
14. Ramos, P. *et al.* Microphysiological systems to study colorectal cancer: State-of-the-art. *Biofabrication* **15**, 032001, DOI: 10.1088/1758-5090/acc279 (2023).
15. Wang, J., Wu, X., Zhao, J., Ren, H. & Zhao, Y. Developing Liver Microphysiological Systems for Biomedical Applications. *Adv. Healthc. Mater.* 2302217, DOI: 10.1002/adhm.202302217 (2023).
16. Achilli, T.-M., Meyer, J. & Morgan, J. R. Advances in the formation, use and understanding of multi-cellular spheroids. *Expert. opinion on biological therapy* **12**, 1347–1360, DOI: 10.1517/14712598.2012.707181 (2012).
17. Chen, B. *et al.* High-throughput acoustofluidic fabrication of tumor spheroids. *Lab on a Chip* **19**, 1755–1763, DOI: 10.1039/C9LC00135B (2019).

18. Tevlek, A., Kecili, S., Ozcelik, O. S., Kulah, H. & Tekin, H. C. Spheroid Engineering in Microfluidic Devices. *ACS Omega* DOI: 10.1021/acsomega.2c06052 (2023).

19. Nagamoto, Y. *et al.* Transplantation of a human iPSC-derived hepatocyte sheet increases survival in mice with acute liver failure. *J. Hepatol.* **64**, 1068–1075, DOI: 10.1016/j.jhep.2016.01.004 (2016).

20. Chen, S. *et al.* Hepatic spheroids derived from human induced pluripotent stem cells in bio-artificial liver rescue porcine acute liver failure. *Cell Res.* **30**, 95–97, DOI: 10.1038/s41422-019-0261-5 (2020).

21. Ten Dam, M. J. M., Frederix, G. W. J., Ten Ham, R. M. T., van der Laan, L. J. W. & Schneeberger, K. Toward Transplantation of Liver Organoids: From Biology and Ethics to Cost-effective Therapy. *Transplantation* DOI: 10.1097/TP.0000000000004520 (2023).

22. Christoffersson, J. & Mandenius, C.-F. Using a Microfluidic Device for Culture and Drug Toxicity Testing of 3D Cells. *Methods Mol. Biol. (Clifton, N.J.)* **1994**, 235–241, DOI: 10.1007/978-1-4939-9477-922 (2019).

23. Sasikumar, S., Chameettachal, S., Kingshott, P., Cromer, B. & Pati, F. 3D hepatic mimics – the need for a multicentric approach. *Biomed. Mater.* **15**, 052002, DOI: 10.1088/1748-605X/ab971c (2020).

24. Bruus, H. Acoustofluidics 7: The acoustic radiation force on small particles. *Lab on a Chip* **12**, 1014, DOI: 10.1039/c2lc21068a (2012).

25. Olofsson, K., Hammarström, B. & Wiklund, M. Ultrasonic Based Tissue Modelling and Engineering. *Micromachines* **9**, DOI: 10.3390/mi9110594 (2018).

26. Jeger-Madiot, N. *et al.* Self-organization and culture of Mesenchymal Stem Cell spheroids in acoustic levitation. *Sci. Reports* **11**, 8355, DOI: 10.1038/s41598-021-87459-6 (2021).

27. Rabiet, L. *et al.* Acoustic levitation as a tool for cell-driven self-organization of human cell spheroids during long-term 3D culture. *Biotechnol. Bioeng.* **121**, 1422–1434, DOI: 10.1002/bit.28651 (2024).

28. Coakley, W. *et al.* Cell-cell contact and membrane spreading in an ultrasound trap. *Colloids Surfaces B: Biointerfaces* **34**, 221–230, DOI: 10.1016/j.colsurfb.2004.01.002 (2004).

29. Khedr, M. M. S. *et al.* Generation of functional hepatocyte 3D discoids in an acoustofluidic bioreactor. *Biomicrofluidics* **13**, 014112, DOI: 10.1063/1.5082603 (2019).

30. Ramaiahgari, S. C. *et al.* From the Cover: Three-Dimensional (3D) HepaRG Spheroid Model With Physiologically Relevant Xenobiotic Metabolism Competence and Hepatocyte Functionality for Liver Toxicity Screening. *Toxicol. Sci.* **159**, 124–136, DOI: 10.1093/toxsci/kfx122 (2017).

31. Wiklund, M. Acoustofluidics 12: Biocompatibility and cell viability in microfluidic acoustic resonators. *Lab on a Chip* **12**, 2018–2028, DOI: 10.1039/C2LC40201G (2012).

32. Du, M. *et al.* The impact of low intensity ultrasound on cells: Underlying mechanisms and current status. *Prog. Biophys. Mol. Biol.* DOI: 10.1016/j.pbiomolbio.2022.06.004 (2022).

33. Organization, W. H. Recommendations for the evaluation of animal cell cultures as substrates for the manufacture of biological medicinal products and for the characterization of cell banks. WHO Technical Report Series WHO TRS N°978, World Health Organization (2013).

34. Ng, S., Gisonni-Lex, L. & Azizi, A. New approaches for characterization of the genetic stability of vaccine cell lines. *Hum. Vaccines & Immunother.* **13**, 1669–1672, DOI: 10.1080/21645515.2017.1295191 (2017).

35. Guillouzo, A. *et al.* The human hepatoma HepaRG cells: A highly differentiated model for studies of liver metabolism and toxicity of xenobiotics. *Chem. Interactions* **168**, 66–73, DOI: 10.1016/j.cbi.2006.12.003 (2007).

36. van der Mark, V. A. *et al.* Stable Overexpression of the Constitutive Androstane Receptor Reduces the Requirement for Culture with Dimethyl Sulfoxide for High Drug Metabolism in HepaRG Cells. *Drug Metab. Dispos.* **45**, 56–67, DOI: 10.1124/dmd.116.072603 (2017).

37. Yosioka, K. & Kawasima, Y. Acoustic radiation pressure on a compressible sphere. **5**, 167–173 (1955).

38. Settnes, M. & Bruus, H. Forces acting on a small particle in an acoustical field in a viscous fluid. *Phys. Rev. E* **85**, 016327, DOI: 10.1103/PhysRevE.85.016327 (2012).

39. Dumy, G. *et al.* Acoustic manipulation of dense nanorods in microgravity. **32**, 1159–1174, DOI: 10.1007/s12217-020-09835-7 (2020).

40. Pazos Ospina, J. F. *et al.* Particle-size effect in airborne standing-wave acoustic levitation: Trapping particles at pressure antinodes. *Phys. Rev. Appl.* **18**, 034026, DOI: 10.1103/PhysRevApplied.18.034026 (2022).

41. Jeger-Madiot, N. *et al.* Controlling the force and the position of acoustic traps with a tunable acoustofluidic chip: Application to spheroid manipulations. *The J. Acoust. Soc. Am.* **151**, 4165, DOI: 10.1121/10.0011464 (2022).

42. Dron, O. & Aider, J.-L. Varying the agglomeration position of particles in a micro-channel using Acoustic Radiation Force beyond the resonance condition. *Ultrasonics* **53**, 1280–1287, DOI: 10.1016/j.ultras.2013.03.012 (2013).

Acknowledgements

We thank Biopredic International for having kindly provided the HepaRG cell line, Dr. Niclas Setterblad and the Technological Core Facility of the Saint-Louis Research Institute, and the Fondation Rothschild for their material and technical support. We thank Dr. Sabine Gerbal-Chaloin, Dr. Martine Daujat and Laurence Françoise for their implications in this study. We thank Dr. Stéphane Brunet for his lecture and advice on the manuscript presentation. We are grateful to Ecole Doctorale Frontières de l'Innovation en Recherche et Education (ED FIRE) – Programme Bettencourt and Université Paris-Cité for the funding of the L. Rabiet thesis. We also thank the Région Ile-de-France (DIM ELICIT) and the French National Research Agency (RHU program ANR-16-RHUS-0005) for providing financial support for this research.

Author contributions statement

L.R., L.A., N.J., D.RG., L.T., G.T., S.K., R.A., J.L. and J-L.A. conceived and planned the experiments. L.R., L.A., N.J., D.RG., L.T., G.T., S.K. and R.A. performed the experiments. J-L.A., J.L. and L.A. supervised the project. All authors discussed the results and contributed to the final manuscript.

Data availability statement

The datasets generated during and/or analysed during the current study are available from the corresponding author on reasonable request.

Additional information

Competing interests

The author(s) declare no competing interests.